HAL open science

# Rheological properties of suspensions of the green microalga Chlorella vulgaris at various volume fractions

Antoine Soulies, Jérémy Pruvost, Jack M Legrand, Cathy Castelain, Teodor Burghelea

## To cite this version:

Antoine Soulies, Jérémy Pruvost, Jack M Legrand, Cathy Castelain, Teodor Burghelea. Rheological properties of suspensions of the green microalga Chlorella vulgaris at various volume fractions. Rheologica Acta, 2013, 52 (6), pp.589-605. 10.1007/s00397-013-0700-z . hal-02534134

**HAL Id: hal-02534134**

**https://hal.science/hal-02534134v1**

Submitted on 20 Mar 2023

**HAL** is a multi-disciplinary open access archive for the deposit and dissemination of scientific research documents, whether they are published or not. The documents may come from teaching and research institutions in France or abroad, or from public or private research centers.

L'archive ouverte pluridisciplinaire **HAL**, est destinée au dépôt et à la diffusion de documents scientifiques de niveau recherche, publiés ou non, émanant des établissements d'enseignement et de recherche français ou étrangers, des laboratoires publics ou privés.

**Rheologica Acta manuscript No.**
(will be inserted by the editor)

# Rheological properties of suspensions of the green micro-alga *Chlorella vulgaris* at various volume fractions

**Antoine Soulies · Jeremy Pruvost · Jack Legrand · Cathy Castelain · Teodor I. Burghelea**

Received: date / Accepted: date

**Abstract** A systematic study of the rheological properties of solutions of non-motile microalgae (*Chlorella Vulgaris* CCAP 211-19) in a wide range of volume fractions is presented. As the volume fraction is gradually increased, several rheological regimes are observed. At low volume fractions (but yet beyond the Einstein diluted limit) the suspensions display a Newtonian rheological behaviour and the volume fraction dependence of the viscosity can be well described by the Quemada model [Quemada(1997)]. For intermediate values of the volume fraction a shear thinning behaviour is observed and the volume fraction dependence of the viscosity can be described by the Simha model[Simha(1952)]. For the largest values of the volume fraction investigated an apparent yield stress behaviour is observed. Increasing and decreasing stress ramps within this range of volume fractions indicate a thixotropic behaviour as well.

The project was supported by the PERLE2 (Pôle Émergent pour la Recherche Ligèrienne en Énergie) program funded by the *Pays de la Loire* district, France.

Antoine Souiles
LUNAM Université, Université de Nantes, CNRS, GEPEA UMR-6144, Bd. de l'Université, CRTT-BP 406, 44602 Saint-Nazaire Cedex, France
E-mail: antoine.soulies@etu.univ-nantes.fr

Jack Legrand
LUNAM Université, Université de Nantes, CNRS, GEPEA UMR-6144, Bd. de l'Université, CRTT-BP 406, 44602 Saint-Nazaire Cedex, France
E-mail: jack.legrand@univ-nantes.fr

Jeremy Pruvost
LUNAM Université, Université de Nantes, CNRS, GEPEA UMR-6144, Bd. de l'Université, CRTT-BP 406, 44602 Saint-Nazaire Cedex, France
E-mail: jeremy.pruvost@univ-nantes.fr

Cathy Castelain
LUNAM Université, Université de Nantes, CNRS, Laboratoire de Thermocinétique, UMR 6607, La Chantrerie, Rue Christian Pauc, B.P. 50609, F-44306 Nantes Cedex 3, France
emailCathy.Castelain@univ-nantes.fr

Teodor I. Burghelea
LUNAM Université, Université de Nantes, CNRS, Laboratoire de Thermocinétique, UMR 6607, La Chantrerie, Rue Christian Pauc, B.P. 50609, F-44306 Nantes Cedex 3, France
E-mail: Teodor.Burghelea@univ-nantes.fr

The rheological behaviour observed within the high concentration regime bears similarities with the measurements performed by Heymann et al. [Heymann and Aksel(2007)] on Polymethyl Methacrylate(PMMA) suspensions: irreversible flow behaviour (upon increasing/decreasing stresses), dependence of the flow curve on the characteristic time of forcing (the averaging time per stress values). All these findings indicate a behaviour of the microalgae suspensions similar to that of suspensions of rigid particles.

A deeper insight into the physical mechanisms underlying the shear thinning and the apparent yield stress regime is obtained by an in-situ analysis of the microscopic flow of the suspension under shear. The shear thinning regime is associated to the formation of cell aggregates (flocs).

Based on the Voronoi analysis of the correlation between the cell distribution and cell sizes, we suggest that the repulsive electrostatic interactions are responsible for this microscale organisation. The apparent yield stress regime originates in the formation of large scale cell aggregates which behave as rigid plugs leading to a *maximally random jammed states*.

**Keywords** microalgue · yielding · jamming

**PACS** PACS 83.60.La · PACS 83.85.Jn · PACS 83.85.Ei · 83.85.Cg.

## Contents

1 Introduction . . . . . 6
2 Experimental methods . . . . . 7
3 Results . . . . . 12
4 Conclusions, outlook . . . . . 26

## List of Figures

1 (a) Micrograph of a *Chlorella* suspension (b) Probability distribution function of the cell radius. The full line is a log-normal fit. . . . . 9

2 Micrographs of *Chlorella* suspensions at various volume fractions indicated in the inserts. The images have been acquired in a quiescent state (no stresses are applied onto the sample). . . . . 10

3 **(a)** Schematic view of the Rheoscope module: **CCD** - digital camera, $M_1, M_2$ - mirrors, **EP** - eye piece, **MO** - microscope objective, **WLS** - white light source, **CL** - collimating lens, **GP** - glass plate, **S** - *Chlorella* sample, **GP** -glass plate, **C** - cone. **(b)** Schematic representation of the increasing/decreasing controlled stress ramp. $N$ is the total number of steps of the ramp and $t_0$ is the time corresponding to each step (the characteristic forcing time). . . . . 11

4 Stress dependence of the viscosity of the microalgal suspension measured in a controlled stress mode for several volume fractions: ($\bigtriangledown$) - $\Phi_v = 0.082$, ($\diamondsuit$) - $\Phi_v = 0.165$, ($\bigcirc$) - $\Phi_v = 0.556$. For each stress value the viscosity data has been averaged for a time $t_0 = 15\ s$. The full line $(-)$ is a fit according to the Cross model, the dashed line $(--)$ is a fit according to the Herschel-Bulkley model. . . . . 13

5 **(a)** The micrograph presented in Fig. 2(c) together with the contours of individual cells detected via image segmentation. **(b)** The corresponding Voronoidiagram correspondingtothemicrographpresentedin Fig. 2(c). . . 14

6 Micrograph acquired during a controlled stress ramp (see Fig. 3(b)) corresponding to $\tau = 0.02 Pa$ and a volume fraction within the **ST** regime ($\Phi_v = 0.15$). The bright patches correspond to agglomerations of cells (flocs) that strongly scatter the light. . . . . 15

7 **(a)** Micrograph of a *Chlorella* suspension with a volume fraction $\Phi_v = 0.556$ (the **YS** regime) sheared at a stress $\tau = 0.02\ Pa$. The time averaged velocity field obtained via the **DPIV** method is overlapped onto the image. **(b)** The corresponding time-averaged mean velocity field (the false colour map) and the time averaged velocity vectors. The closed curves superposed to each panel highlight the solid-like agglomerations of *Chlorella* cells. . . . . 19

8 Dependence of the relative viscosity of the microalgal suspension $\eta_r$ on the volume fraction of the microalgue $\Phi_V$. The dashed line is a fit according to the Quemada model [Quemada(1997)] and the full line is a fit according to the Simha model, [Simha(1952)]. The labels indicate the experimentally observed rheological regimes: **N** - Newtonian, **ST** - shear thinning, **YS** -yield stress. Within the **ST** and **YS** regimes, the relative viscosity has been measured at a fixed stress, $\tau = 1 Pa$.

9 Dependence of the onset of the shear thinning behavior $\tau_0$ measured within the **ST** regime and of the apparent yield stress $\tau_y$ on the volume fraction $\Phi_V$. The labels indicate the experimentally observed rheological regimes: **N** . . . . . 19

Newtonian, **ST** - shear thinning, **YS** - yield stress . . . . . 21

10 Viscosity measurements within the intermediate concentration regime at a volume fraction $\Phi_v = 0.148$ (**ST**, see Fig. 8) for both increasing ($\square$) and decreasing ($\bigcirc$) stress ramp and several values of the characteristic forcing

time: **(a)** $t_0 = 5\ s$ **(b)** $t_0 = 10\ s$ **(c)** $t_0 = 15\ s$ **(d)** $t_0 = 30\ s$. . . . . 23

11 Viscosity measurements within the highly concentrated regime at a volume fraction $\Phi_v = 0.556$ (the **YS** regime, see Fig. 8) for both increasing (□) and decreasing (◯) stress ramp. The characteristic forcing time was $t_0 = 15s$. . 23

12 Dependence of the zero shear viscosity $\eta_0$ (empty symbols) and the ter--minal viscosity $\eta_{int}$ (full sysmbols) measured within the **ST** regime on the increasing branch of the stress ramp on the characteristic time of forcing $t_0$. The symbols refer to different volume fractions of the microalgae: (□, ■) - $\Phi_v = 0.148$, (◯, ●) - $\Phi_v = 0.165$, (△, ▲) - $\Phi_v = 0.181$. . . . . 25

13 Dependence of the viscosity of a highly concentrated suspension (within the **YS** rheological regime, ) measured at a fixed stress on the characteristic forcing time. The symbols refer to stress value: (◯) - $\tau = 0.1Pa$, (●) - $\tau = 10Pa$.The volume fraction is $\Phi_v = 0.37$. . . . . 26

## List of Tables

1 Range of the volume fractions of the *Chlorella* solutions investigated. $C_x^{rms}$ and $\Phi_v^{rms}$ stand for the root mean square deviation (rms) of the dry weight concentration and of the volume fraction, respectively. . . . . 9

## 1 Introduction

Microalgae are photosynthetic aquatic microorganisms. Their biodiversity enables to produce various compounds (proteins, pigments, lipids, etc.) having potential applications in a wide range of domains such as food-processing industry [Becker(2007)], cosmetics, pharmaceutics, green chemistry or energetic industry [Mouget and Tremblin(2002), Mata et al(2010), Satyanarayana et al(2011)]. *Chlorella Vulgaris*, a non motile unicellular non-flagellated green micro-alga is, undoubtedly, one of the major species cultivated at an industrially relevant scale. This is because of its easy growth and of its commercial potential, mainly for nutrition related purposes [Spolaore et al(2006)], due to its high content in proteins (60%), polysaccharide (20%), carotenoids, vitamins, unsaturated fatty acids (15%) [Basu et al(2001)Basu, Vecchio, Flider, and Orthoeter] and lutein for food complements [Shi et al(1997)]. Its robustness enables its exploitation in a broad diversity of systems, ranging from open ponds to photobioreactor technology (closed systems) [Richmond(2004), Carvalho et al(2006), Ugwu et al(2008), Lehr and Posten(2009), Pandey et al(2011)].

Due to a high degree of control of the culture conditions, the photobioreactor technology allows a higher productivity. With an appropriate engineering and operating protocol, a high cell density culture (i.e., high biomass concentration) can especially be obtained. Hydrodynamics is one of the key aspects when working in high-cell density culture.High-cell density cultures are indeed obtained in systems having a very high ratio between the illuminated surface and the culture volume, which translates into a shallow depth, typically smaller than $0.01m$ [Cornet(2010), Pandey et al(2011), Doucha et al(2005)]. The high degree of confinement com-bined with a high biomass concentration tends to decrease the mixing performances which can have several negative impacts on the process: a decrease of the efficiency of the mass transfer, an increase in the risk of biofilm formation and a less efficient light conversion in the systems due to smaller displacement of flowing cells along the light gradient in the culture volume.

A high degree of optimisation of the hydrodynamic conditions requires a proper un-derstanding of the rheological behaviour of the suspension of cells. There exist, however, very few studies regarding the rheological properties of suspensions of microalgae, partic-ularly in the context of high-cell density culture conditions with dry biomass concentration ($> 10kg\ m^{-3}$).

A rheological characterisation of microalgae slurries at various mass concentrations has been recently presented by Wileman et al. [Wileman et al(2011)]. Depending on the microalgae concentration, they identify either a Newtonian behaviour within the dilute regime or a shear-thinning behaviour (characterised by a power law stress rate of strain dependence) within the semi-dilute regime. No apparent yield stress behaviour is reported and the reversibility of the deformation states upon increasing/decreasing stresses was not investigated.

Adesanya and coworkers have recently performed an experimental study of the rheological behaviour of suspensions of *Scenedesmus obliquus* micro-alga at various volume fractions up to 0.15%, [Adesanya et al(2012)].

Using the piezoaxial vibrator **(PAV)** technique which allowed one to measure the complex viscosity $\eta^*$ at various frequencies, they observe a deviation from the Cox-Merz rule corresponding to the high volume fraction regime. By a separate microscopical visualisation of the micro-algae suspensions, they relate this effect to the formation of cell aggregates (flocs) which they claim it is due to attractive van der Waals forces. Up to the maximal vol-

ume fraction they have investigated, they do not observe yield stress effects. This may be due to the rather limited value of the maximal volume fraction they have investigated.

The study of the dependence of the viscosity of a solution of *Chlorella pyrenoidosa* by Wu et al reveals a yield stress at large volume fractions, [Wu and Shi(2008)]. The yield stress behaviour of high volume fraction *Chlorella* suspensions remains, however, largely unexplored.

As *Chlorella* microalgae have a roughly spherical shape with radii of the order of several microns and a supposedly rigid membrane [Northcote and Goulding(1958), Takeda(1988), Kapaun and Reisser(1995)] it appears natural to attempt to understand the rheological be-haviour of suspensions of these micro-organisms within the general framework of the rhe-ology of suspensions of rigid particles.

As opposed to the rheology of *Chlorella* microalgae suspensions which, to our best knowledge, is still poorly documented an important and detailed body of literature (both theoretical and experimental) can be found on the rheology of suspensions of rigid particles.

A comprehensive review of these studies can be found in both the *Springer Handbook of Experimental Fluid Dynamics*, [Tropea et al(2007)], and in a more recent textbook, [Wagner(2011)]. A systematic study of the shear thinning behaviour of intermediately concentrated suspensions of rigid particles is presented by Kruif and his coworkers, [de Kruif et al(1985)].

The volume fraction correlation of the yield stress behavior of concentrated suspensions has been recently investigated by Mueller and his coworkers, [Mueller et al(2010)].
A detailed experimental investigation of the yield stress behavior of concentrated suspensions of polymethylmetacrylate (PMMA) was reported by Heymann and Aksel, [Heymann and Aksel(2007)]. A major finding of their work is that, except for the fluid deformation regime, the deformation states are not recoverable upon an increase/ decrease of the applied stresses and a clear hysteresis is observed.

The global aim of this study is to investigate in depth the rheological properties of *Chlorella Vulgaris* suspensions in a wide range of volume fractions and externally applied stresses.

The paper is organised as follows. The description of the experimental methods is presented in Sec. 2 and includes the description of the preparation protocol of the suspensions of microalgae Sec. 2.1 and the rheological procedures employed in characterising the suspensions, Sec. 2.2.

The experimental results are presented in Sec. 3. The rheological regimes corresponding to various volume fractions of the suspension are described in Sec. 3.1.

The reversibility of the deformation states and the time dependence of the rheological properties within each of these regimes are investigated in Sec. 3.2.

The paper closes with a brief discussion of the main conclusions of our experiments and the impact of our findings on future theoretical, numerical and experimental investigation of *Chlorella* suspensions, Sec. 4.

## 2 Experimental methods

### 2.1 Preparation of the *Chlorella* microalgae suspensions

*Chlorella* microalgae were grown in a bubble column photobioreactor (volume of 0.12 $m^3$, diameter of 0.57 $m$ and specific illuminated area 3.5 $m^2$). Each culture was illuminated with

an incident photon flux density (PFD) of around 150 $\mu mole_{h\nu} m^2\ s^{-1}$ (white light). The culture medium was composed of (in g/l) $NH_4Cl$, 1.45, $MgSO_4.7H_2O$, 0.28, $CaCl_2.2H_2O$, 0.05, $KH_2PO_4$, 0.61, $NaHCO_3$, 1.68 and 0, 5$ml\ l^{-1}$ of Hutner solution (trace elements, see Ref. [Harris(1989)] for a complete description). The *Chlorella* suspensions, once collected, were artificially concentrated by centrifugation (15 minutes at 5000 $g$). The dry biomass concentration $C_x$ of the concentrate was then measured. Filters (glass micro-fiber filters, GF/F Whatman) with 0.22 micrometer pore size were dried during 24 hours in a 100$^oC$ oven. They were then weighted and used to filter a known volume of algal suspension. The filters were finally placed for 24 hours in a 100$^oC$ oven and re-weighted. This duration was sufficient to obtain a complete drying. The weight difference was finally used to calculate the dry biomass concentration of the concentrate. A range of samples of known concentration (here expressed in volume fraction, $\Phi_v$) was then prepared by diluting the concentrated wet suspension with the supernatant previously removed. The volume fraction ($\Phi_v$) was determined from the dry weight concentration following the relations below:

$$\Phi_v = \frac{C_x}{\rho_W w_D} \tag{1}$$

$$\rho_W = x_W \rho_0 + (1 - x_W)\rho_D \tag{2}$$

In the equations above $\rho_W$ and $\rho_D$ stand for the density of the wet and dry biomass, respectively and $\rho_0$ is density of the water. $w_D = \frac{(1-x_W)\rho_D}{\rho_W}$ stands for the mass fractional content in dry solid in the microalgae and $x_W$ is the water fractional content in wet microalgae (both quantities are non-dimensional).

The water mass content $x_w$ and density of dry biomass $\rho_D$ necessary for the calcula-tion were respectively 0.82 and 1400 $kgm^{-3}$, as proposed in Ref. [Cornet(2010)] who found those values nearly constant among various microorganisms including microalgae and bacteria.

The range of investigated volume fractions is given in Table 1 (because it is a usual parameter in the field of microalgae cultivations, dry weight concentrations are also given).

It is very important to note Table 1 that the range of volume fractions we have explored is significantly broader than the ranges previously explored by others see for example Ref. [Adesanya et al(2012)]. This allows us to provide a more complete description of the rheological behaviour of *Chlorella* microalgae.

The maximum packing fraction corresponding to a *maximally random jammed state* is $\Phi_v = 0.637$ ($C_x = 159.25\ g/l$).

Microalgae generally produce Exo-Poly Saccharides and Extracellular Polymeric Substances (EPS) in order to mitigate a physiologic stress (related to either nutrient or light) or a mechanical stress. We also note that EPS favors biofilm and floc formation. The volume fraction calculation presented above was solely based on the mass of the *Chlorella* cells.

To characterise size distribution of microalgae, a set of 165 images comprising 2873 cells were acquired using a digital colour camera (Axio Cam MRc third version, 1.4 megapix-els, 12 bit quantisation) mounted on Zeiss upright microscope (Zeiss Axio Scope $A_1$). The microscope is equipped with an objective with 20$X$ magnification and a depth of field of 5.8 $\mu m$. The contour of each cell was extracted from each image using a commercial image processing software (Axio vision routine) and the radii of the cells were determined. The analysis of the shape of the *Chlorella* cells is illustrated in Fig. 1. Cells were found of a roughly spherical shape (see Fig. 1 (a)) with a mean radius $r_0 = 1.98\mu m$ and a standard deviation of $r^{std} = 0.41\mu m$. Cells size distribution (radii) can be modelled by a log-normal

**Table 1** Range of the volume fractions of the *Chlorella* solutions investigated. $C_x^{rms}$ and $\Phi_v^{rms}$ stand for the root mean square deviation (rms) of the dry weight concentration and of the volume fraction, respectively.

| $\mathbf{C_x}(\mathbf{g/l})$ | $\mathbf{C_x^{rms}}(\mathbf{g/l})$ | $\Phi_v(\%)$ | $\Phi_v^{rms}(\%)$ |
|---|---|---|---|
| 147 | 4.74 | 58.3 | 1.88 |
| 92 | 1.8 | 36.5 | 0.71 |
| 62.5 | 2.28 | 24.8 | 0.9 |
| 58.3 | 2.24 | 23.1 | 0.89 |
| 54.2 | 2.08 | 21.5 | 0.82 |
| 50 | 1.92 | 19.8 | 0.76 |
| 45.8 | 1.76 | 18.2 | 0.7 |
| 37.5 | 1.44 | 14.9 | 0.57 |
| 29.2 | 1.12 | 11.6 | 0.44 |
| 20.8 | 0.8 | 8.3 | 0.31 |
| 12.5 | 0.48 | 5 | 0.19 |
| 4.2 | 0.16 | 1.7 | 0.06 |

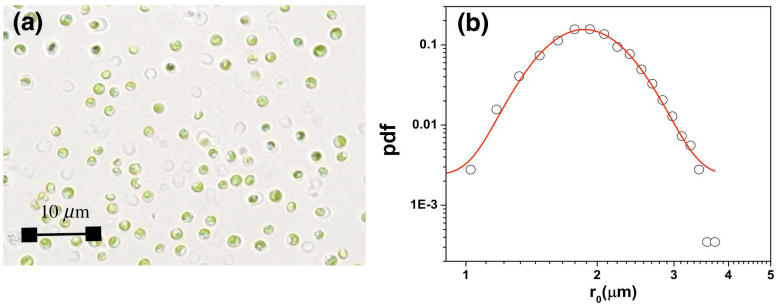


**Fig. 1** (a) Micrograph of a *Chlorella* suspension (b) Probability distribution function of the cell radius. The full line is a log-normal fit.

distribution (the full line in Fig. 1 (b)) as already observed elsewhere for *Chlamydomonas Reinhardtii* species which was found almost similar in shape [Pottier(2005)]. It must be noticed that the rather large cell size makes *Chlorella* suspensions to fall into the class of non-Brownian suspensions.

To get a deeper insight into the microstructure of *Chlorella* suspensions, we present in Fig. 2 micrographs of such suspensions at various volume fractions (indicated in the inserts). Note that the micrographs have been acquired in a quiescent state (no flow).

At low volume fractions ($\Phi_v = 5.4\%$ panel (a) in Fig. 2), a dilute regime is observed and no apparent organisation of the cells is observed. As the volume fraction is increased ($\Phi_v = 16.2\%$ panel (b) in Fig. 2) an apparent reorganisation of the *Chlorella* cells can be observed at a close inspection: the larger cells tend to group together and voids (regions free of cells) can be observed as well. As the volume fraction is increased even further,($\Phi_v = 37.8\%$ panel (c) in Fig. 2) the organisation of the *Chlorella* cells becomes more obvious. The cells are organised in flocs and individual flocs are interconnected by ”bridges” formed by smaller cells. Within the highly concentrated regime, ($\Phi_v = 48.6\%$ panel (d) in Fig. 2) a highly dense and randomly packed cell structure is observed (although we could not identify individual cells within the high volume fraction micrographs a simple visual inspection reveals no particular arrangements of individual cells). Within this state, the cells come into contact consistently with a jammed particle system.

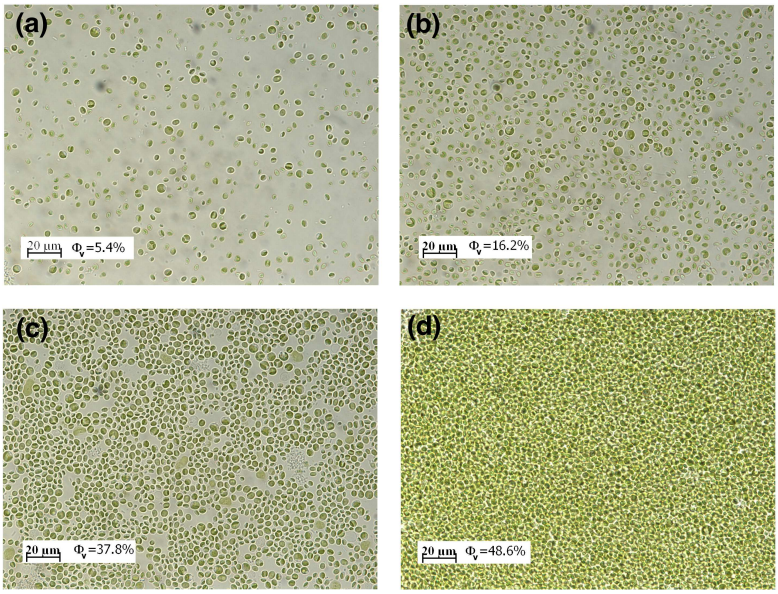


**Fig. 2** Micrographs of *Chlorella* suspensions at various volume fractions indicated in the inserts. The images have been acquired in a quiescent state (no stresses are applied onto the sample).

We note that, from an industrial stand point, it is precisely this regime of high volume fractions that presents a high practical interest (high cell density photobioreactor).

## 2.2 Rheological measurements

The rheological characterisation of the microalgae solutions has been performed on a Haake Mars *III* rotational rheometer (Thermo Fisher Scientific, Karlrsruhe, Germany) equipped with a nano-torque module. The nano-torque module allows accurate rheological measurements of dilute samples in a range of low applied shear stresses.

The measurements have been performed using a cone-plate geometry ($R = 60\ mm$ radius and $2deg$ angle). Prior to each rheological test, the samples have been carefully loaded paying attention to the reproducibility of the shape of the free meniscus in subsequent experiments. To prevent the evaporation of the sample during long tests, the fluid meniscus has been covered by a protective thin film of silicone oil. Additionally, the entire geometry has been enclosed in a bell-shaped chamber made of a thermally insulating material (teflon).

All the experiments reported in this paper have been conducted at the same temperature, $T = 20^oC$.

The minimum torque that could be resolved during our measurements was $T_{min} = 0.01\mu Nm$ which corresponds to a minimum stress $\tau_{min} = 1.76 \cdot 10^{-4} Pa$. The minimum angular speed that could be resolved during our measurements was $\Omega_{min} = 10^{-7} rot/min$ which corresponds to a minimum shear rate $\dot{\gamma}_{min} = 3 \cdot 10^{-7} s^{-1}$. We have made sure that, during of each of the experiments reported in this paper, the applied stresses and measured rates of the stresses and shear rates were larger than the limiting values given above.

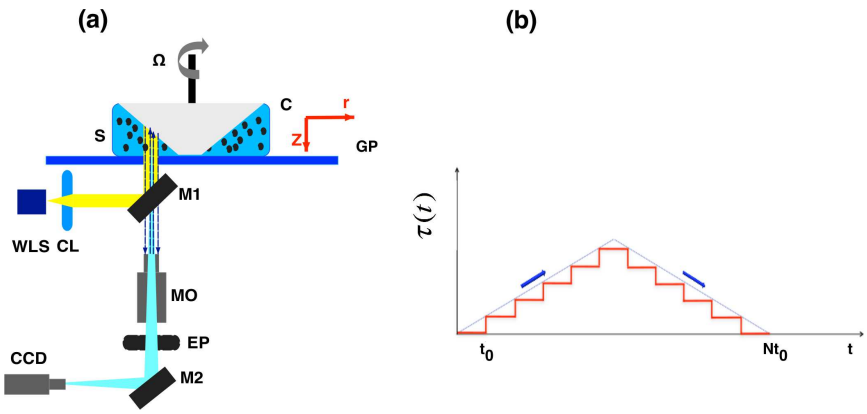


**Fig. 3** **(a)** Schematic view of the Rheoscope module: **CCD** - digital camera, $M_1$,$M_2$ - mirrors, **EP** - eye piece, **MO** - microscope objective, **WLS** - white light source, **CL** - collimating lens, **GP** - glass plate, **S** - *Chlorella* sample, **GP** - glass plate, **C** - cone. **(b)** Schematic representation of the increasing/decreasing controlled stress ramp. $N$ is the total number of steps of the ramp and $t_0$ is the time corresponding to each step (the characteristic forcing time).

The rheometer is also equipped with a Rheoscope module (from ThermoFisher Scien-tific, Karlsruhe, Germany) which allows the visualisation of the microstructure of the suspensions during the rheological tests, 3 (a). A white light beam emitted by the source **WLS** is collimated by the lens **CL** and directed by the mirror $M_1$ onto the sample **S** through the glass plate **GP**. The light reflected by the smooth inner surface of the cone **C** is focused by a microscope objective **MO** ($10X$ magnification and 8.5 $\mu m$ depth of field) and an eye piece **EP** onto the charged coupled device of the digital camera **CCD** ( Chameleon CMLN-13S2M-CS from Point Grey), see Fig.3 (a).

The Rheoscope module is equipped with a motorised focusing system which allows one to acquire flow images at various depths within the sample. A second motorised translational stage allows one to move the focusing point along the radial direction $r$ over a distance of 15 $mm$ measured from the position $r = 0$ $mm$;

It is important to point out that the Rheoscope microscopic visualisation system works in reflection, i.e. the **CCD** camera receives the light reflected by the surface of the cone **C**. This inherently results into a image quality lower than that provided by the classical upright microscope used to visualise the suspensions in quiescent state (i.e. in the absence of a flow), see the description provided in Sec. 2.1 and the micrographs illustrated in Figs. 1(a), 2.

Whereas the quality of the images acquired with the Rheoscope system does not suffice for an accurate identification of individual *Chlorella* cells, two other functionalities of this module have been employed through our study.

Firstly, the ability to focus at any point along the vertical direction $z$ allows one to probe the emergence of the wall slip phenomenon which is of paramount importance for rheology of suspensions, [Buscall(2010)].

Secondly, the acquisition of a sequence of flow imaging and its processing via a standard multi-pass Digital Particle Image Velocimetry (**DPIV**) algorithm (see Refs. [Scarano and Rhiethmuller(2001), Raffel et al(September 2007)] for a comprehensive description of the method) allows in-situ measurements of the velocity distributions which may be be used to indirectly probe the formation of micro-structures of *Chlorella*

cells. For this purpose, a judicious choice of the inter frame of the **CCD** camera together with a appropriate choice of the sequence of interrogation windows (adapted to the magnitude of the cell's displacements in the field of view) allowed one to resolve speeds as small as 0.3 $\mu ms^{-1}$ with an instrumental error better than 6 %. These rather low flow speeds could be successfully resolved due to a additional sub-pixel interpolation routine developed in the house.

For this rheometric flow the Reynolds number can be defined as $Re = \frac{R^2 \Omega \rho}{\eta}$ where $\Omega$ is the angular velocity of the geometry, $\rho$ the density of the suspension and $\eta$ its viscosity. Corresponding to each of the measurements further reported, the Reynolds number $Re$ was of order of unity (or smaller) indicating that inertial effects typically responsible for the emergence of secondary flows were practically absent.

The rheological behaviour of the microalgae suspensions has been assessed by controlled stress flow ramps schematically illustrated in Fig. 3 (b). The time interval $t_0$ corresponding to each step of the ramp was varied in order to probe the sensitivity of the rheological response of the sample to the steadiness of the rheometric flow.

To probe the reversibility of the deformation states, both increasing and decreasing stress ramps have been performed.

## 3 Results

According to the dimensional analysis by Krieger et al. [Krieger and Dougherty(1959)], the relative viscosity of a (mono-disperse) suspension of rigid particles $\eta_r = \frac{\eta}{\eta_0}$ (where $\eta_0$ is the viscosity of the culture medium which is slightly larger than that of the water, $\eta_0 \approx 2mPas$) should satisfy the follow functional dependence:

$$\eta_r = \eta_r(\Phi_v, Pe, De) \tag{3}$$

In the Eq. above, $Pe$ and $De$ stand for the Péclet number and Deborah numbers are defined as $Pe = t_{br}\dot{\gamma}$ and $De = t_{br}/t_0$, respectively. Here $\dot{\gamma}$ is the rate of shear, $t_{br} = \frac{6\pi\eta_0\bar{r}_0^3}{k_B T}$ ($k_B$ is the Boltzmann constant and $T$ the absolute temperature) is a characteristic time scale associated with the Brownian motion and $t_0$ is a time scale associated with the experiment. Whereas the dependence of the relative viscosity on the volume fraction and the Péclet number has been studied by many authors (see Ref. [Tropea et al(2007) for a review of these studies) the dependence on the Deborah number has been much less explored: most of the previous rheological studies report steady state rheological measure-ments, $t_0 \to \infty$ or $De \to 0$. We note, however, that realistic flows of microalgae suspensions in various reactors are not necessarily steady ($t_0$ is finite and $De > 0$) and, to properly model them, the $De$ dependence of the relative viscosity needs to be investigated as well.

The global aim of this study is to explore experimentally the entire functional dependence predicted by Eq. 3.

The volume fraction dependence of the rheological properties of the *Chlorella* suspensions has been assessed by running controlled stress flow ramps for suspension with various volume fractions given in Table 1. By choosing an appropriate range of the applied stresses, for some of the volume fractions listed in Table 1 the Péclet number was varied over nearly three orders of magnitude. For each value of the volume fraction, the Deborah dependence has been investigated by varying the characteristic forcing time $t_0$ during which the stress is maintained constant during the flow ramp. The time dependence of the rheological proper-ties has been further investigated by studying the reversibility of the deformation states by performing increasing and decreasing flow ramps.

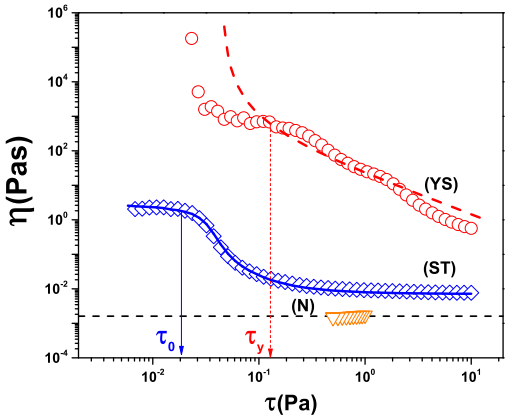


**Fig. 4** Stress dependence of the viscosity of the microalgal suspension measured in a controlled stress mode for several volume fractions: (▽) - $\Phi_v = 0.082$, (◇) - $\Phi_v = 0.165$, (○) - $\Phi_v = 0.556$. For each stress value the viscosity data has been averaged for a time $t_0 = 15\ s$. The full line (–) is a fit according to the Cross model, the dashed line (– –) is a fit according to the Herschel-Bulkley model.

## 3.1 Rheological regimes

To identify various rheological regimes, controlled stress flow ramps have been performed in identical conditions for various microalgae solutions with the cell volume fraction $\Phi_v$ ranging in between 0.016 and 0.556.

Several such measurements are presented in Fig. 4. Within the dilute regime [1] ($\Phi_v \leq 0.115$) no stress dependence of the viscosity is observed (the down-triangles in Fig. 4, (▽)) indicating a Newtonian (**N**) rheological behaviour.

As the volume fraction is increased, an entirely different rheological behavior is ob-served (the rhumbs (◇) in Fig. 4). Corresponding to stress values smaller than a critical value ($\tau \leq \tau_0$) a Newtonian behaviour characterized by a viscosity plateau which defines the zero shear viscosity $\eta_0$ is observed. Beyond this critical stress value ($\tau > \tau_0$) a shear thin-ning rheological behaviour **ST** is observed, $\eta \propto K\dot{\gamma}^{\frac{n-1}{n}}$ where $K$, $n$ stand for the consistency and the power law index, respectively. A second viscosity plateau which defines the infinite shear viscosity $\eta_{inf}$ is observed at large applied stresses.

The viscosity measurements within the **ST** regime may be described over the entire range of rates of shear explored during our measurements by the Cross model (the full line in Fig. 4), [Cross(1965)]:

$$\eta = \eta_{inf} + \frac{\eta_0 - \eta_{inf}}{1 + \alpha\dot{\gamma}^n} \tag{4}$$

Within the framework of the Cross model, the onset of the shear thinning (see the dia-monds in Fig. 4) behaviour may be estimated as $\tau_0 \approx \eta_0 \alpha^{-1/n}$.

The good agreement of the viscosity data acquire within the **ST** volume fraction regime illustrated by the full line in Fig. 4 prompts us to investigate closer the main assumption underlaying the Cross model according to which the low stress viscosity plateau is related to

[1] We note that this regime is yet beyond the Einstein's ultra-dilute limit which was of no particular interest to the present study.

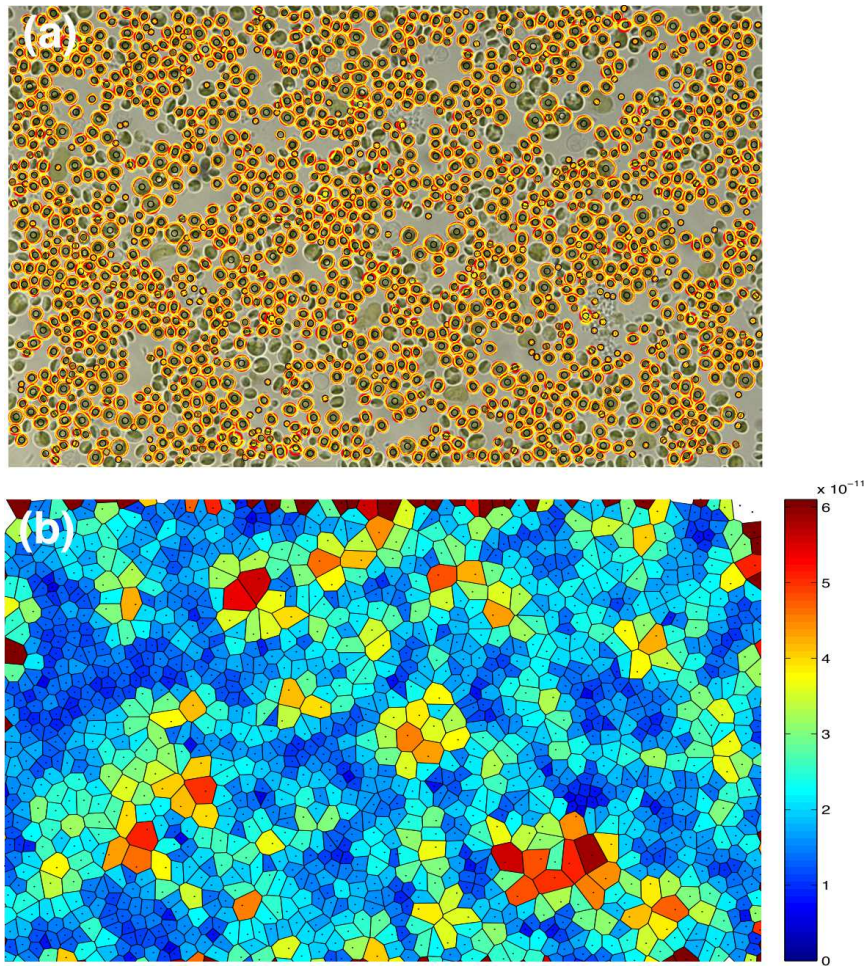


**Fig. 5** **(a)** The micrograph presented in Fig. 2(c) together with the contours of individual cells detected via image segmentation. **(b)** The corresponding Voronoi diagram corresponding to the micrograph presented in Fig. 2(c).

the formation of a flocculated microstructure of individual particles (cells). Although some voids (regions without cells) are clearly visible in Fig. 2(c) an organisation of individual cells in flocculated micro-structures is not obvious. To get a deeper insight into the micro-scale organisation of the *Chlorella* suspension, we have passed this micrograph to a sequence of image processing algorithms implemented under Matlab®able to detect the edge of individual cells, fit their contour by an ellipsis which ultimately gives the coordinates of their centroid and their size. The result of such an analysis is presented in Fig. 5(a). The accuracy of the cell identification is about 5%.

The simultaneous determination of the centroids of the cells and their size (area in the field of view) allows the partition of the field of view in Voronoi polygons. The Voronoi dia-

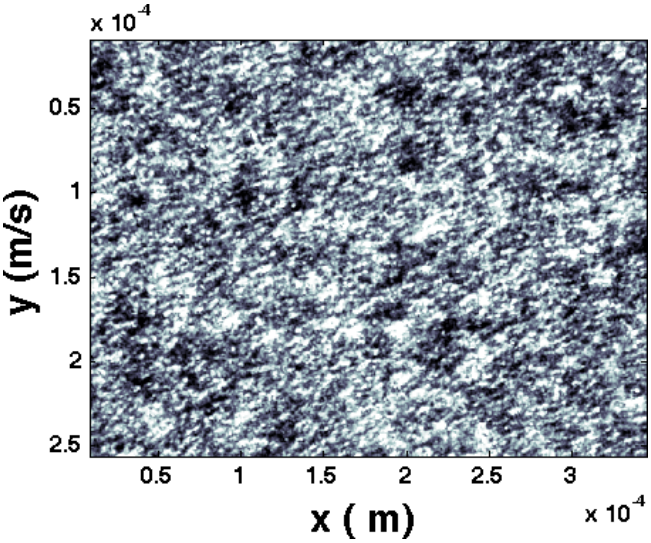


**Fig. 6** Micrograph acquired during a controlled stress ramp (see Fig. 3(b)) corresponding to $\tau = 0.02Pa$ and a volume fraction within the **ST** regime ($\Phi_v = 0.15$). The bright patches correspond to agglomerations of cells (flocs) that strongly scatter the light.

gram consists in the partition of the field of view in convex polygons (equal in number to the number of the detected *Chlorella* cells) such as each polygon contains exactly one centroid of a cell (called in this context generating point) and every point of a given polygon is closer to its generating point than to any other, [de Berg et al(2008)].

The result of the Voronoi triangulation of the micrograph presented in Fig. 5 (a) is presented in Fig. 5 (b).

The false colormap is related to the size of the *Chlorella* cells. The computation of of the Voronoi diagram allows one to visualise the agglomerations (flocs) of cells of similar sizes separated by voids. It is interesting to note that the flocs are mainly constituted of the smallest cells (colour coded in blue, Fig. 5 (b)) whereas the biggest cells (colour coded in red, Fig. 5 (b)) tend to isolate themselves creating voids around them.

This rather unexpected correlation between the spatial distribution of the cells and their sizes may be understood in terms of repulsive interactions between the cells. Indeed, the surface of the *Chlorella* cells is negatively charged, [Kumar et al(1981)] and, assuming that various cells are characterised by similar superficial charge density, it is likely that larger cells repel the small ones leading to the formation of the flocs visible in Fig. 5 (b)). This conclusion is consistent with the experiments of Dibble and his cowork-ers which demonstrated that interparticle short range interactions (attractive, in their case) may lead to a microscopic scale organisation of individual particles in a colloidal dispersion,[Dibble et al(2006)].

As the micrograph presented in Fig. 2(c) and reanalysed in Fig. 5 has been acquired in a quiescent state (absence of flow) the points made above can only be used to understand the rheological behaviour in the limit of vanishing applied stress, $\tau \to 0$.

The natural question that needs to be addressed at this point is whether the microscopic scale organisation of cells in flocs persists under shear at values of the applied stress corresponding to the low shear viscosity plateau visible in Fig. 4 (the rhumbs, (◇)).

To address this question, we resort to the in-situ flow visualisation using the Rheoscope module presented in Fig. 3 (a) and described in Sec. 2.2.

A micrograph of a *Chlorella* suspension with a volume fraction corresponding to the **ST** regime acquired during a controlled stress ramp for $\tau = 0.02\ Pa$ is presented in Fig. 6. Although the quality of this flow image does not fully match the quality of the micrographs acquired in the absence of flow with the table top upright microscope, individual flocs of cells are clearly visible as white colour patches.

Of particular interest within the **ST** regime was the emergence of the wall slip phenomenon which is often encountered during the rheological measurements of intermediately and highly concentrated suspensions, [Buscall(2010)].

The Rheoscope module equally offers a simple and elegant method of directly probing the wall slip by focussing the the microscope objective **MO** at the level of the bottom glass plate **GP** (see Fig. 3 (a)). The direct visual assessment of the micro-flow led us to the conclusion for each of the volume fractions investigated with the **ST** regime the slip velocity at the bottom glass plate **GP** never exceeded 5% of the speed of the rotating cone **C**. This conclusion has been reinforced by additional rheological tests performed with a roughened plate-plate geometry (obtained by gluing sand paper on the parallel plates) which revealed no significant differences in the viscosity curves.

To conclude this part, the micro-structural observation of the *Chlorella* suspension in both a quiescent and sheared state confirms the initial hypothesis that the low stress viscosity plateau observed within the **ST** volume fraction regime is associated to the formation of cell aggregates (flocs) in agreement with the main assumptions of the Cross model [Cross(1965)] and to the more recent theoretical work by Quemada [Quemada(1997)].

As the volume fraction is increased even further, $\Phi_v \geq 0.25$ an apparent yield stress **YS** behaviour can be observed: the low shear stress plateau visible within the **ST** regime degenerates into a viscosity divergence (the circles (◯) in Fig. 4).

We emphasise once more that, to our best knowledge, a yield stress behaviour of suspensions of *Chlorella* has been very little documented by previous experimental studies, [Wu and Shi(2008)].

It is important to note that, based on the resolution of both the torque and angular speed measurements on the Mars III rheometer (see the discussion and figures presented in Sec. 2.2) the rather large values of the viscosity observed in Fig. 4) in a range of low applied stresses remain within the operating range of the device and should not be attributed to instrumental artefacts.

The yield stress behaviour can be quantitatively (but yet formaly) assessed using a Herschel-Bulkley model for the stress-rate of strain dependence, $\tau = \tau_y + K\gamma^n$, where $\tau_y$ stands for the yield stress (see the circles and the dash-dot line in Fig. 4).

It has to be pointed out that, from an industrial perspective, it is precisely the high volume fraction (high cell density culture) regime that presents an industrial interest. The emergence of a apparent yield stress behaviour within this volume fraction regime might actually change most of what we thought we know about the impact of both the rheology and the hydrodynamics on the design of efficient photobioreactors. Namely, a viscosity divergence would naturally lead to the emergence of a unmixed plug flow regions or stagnant volumes in flow regions characterised by a low shear rate.

Such non-trivial hydrodynamic effects triggered by a still insufficiently understood rheological behaviour would certainly render the commercially available numerical tools com-

monly used to ”design” an efficient mixing protocol useless and new ones would have to be developed. This motivates us to pay a particular attention to the high volume fraction **YS** regime.

A fundamental question that needs to be addressed is: *What are the underlying physical mechanisms behind the experimental observation of an apparent yield stress behaviour during slow shear flows of Chlorella suspensions?*

Jaishankar and his coworkers observed an apparent (bulk) yield stress behaviour in a solution of Bovine Serum Albumin (BSA) under shear, [Jaishankar et al(2011)].

They have elegantly demonstrated that the apparent yield stress exhibited by these solutions originates in the presence of a viscoelastic layer formed due to the adsorption of protein molecules at the air-water interface in the rheometric geometry. The elastic origins of the apparent bulk yield stress behaviour was unequivocally demonstrated by creep tests per- formed at various applied constant stresses which revealed an oscillatory behaviour of the creep compliance at short times known in the literature as the *creep ringing* phenomenon. Moreover, they have demonstrated that addition of a surfactant (Tween 80) which inhibits the protein adsorption at the interface may diminish and even entirely suppress the apparent yield stress behaviour turning the BSA solution into a Newtonian fluid (see Figs. 9 and 11 in Ref. [Jaishankar et al(2011)]).

It is known that the *Chlorella* micro-alga is reach in proteins, which justifies its potential importance to the food industry. However, these proteins are part of the intracellular matter and, unless the cell are mechanically or chemically damaged, they are not expected to be be found in the culture medium. As our suspensions consisted of living change, we do not expect that the mechanism underlying the apparent yield stress behaviour is the same as in Ref. [Jaishankar et al(2011)]).

To probe this, however, rheological measurements performed on the culture medium itself (the cells have been eliminated via centrifugation) revealed a Newtonian behaviour (a viscosity constant with the applied stress).

Additional creep tests performed at low applied stresses and volume fractions $\Phi_v$ within the **YS** regime revealed no *creep ringing* phenomenon (data not shown here).

These tests demonstrate that, unlike in the case of the experiments reported by Jaishankar and his coworkers in Ref. [Jaishankar et al(2011)]), the apparent yield stress behaviour observed in Fig. 4 is not related to an interfacial elasticity effect and, most probably, its physical origins should be investigated in relation to the bulk microscopic organisation of individual cells under shear.

It is equally known that an apparent yield stress behaviour may emerge in particle systems via both a jamming and a glass transition. A recent theoretical study by Ikeda and his coworkers points out the difficulty of separating the two contributions in a practical setting as well as a non-negligible level of ambiguity of the interplay between the glass and jamming transition existing in the rheological literature, [Ikeda et al(2012)]. A theoretical suggestion of how the two contributions can be separated based on the careful correlation of the nonlinear rheological data with the unified jamming diagram initially proposed by Liu and Nagel (see Ref. [Liu and Nigel(1998)]) in the space $(\eta_r, \Phi_v, T)$ is proposed in Ref. [Ikeda et al(2012)].

As all of our rheological measurements have been performed at a constant temperature $T$, we can not reconstruct a three dimensional jamming diagram and resort to the conceptual framework proposed in Ref. [Ikeda et al(2012)].

To get a deeper physical insight into the origins of the apparent yield stress behaviour observed in Fig. 4 (the circles (◯)) we turn our attention to the microscopic scale organisation of the *Chlorella* suspension within this range of volume fractions.

The micrograph of a $\Phi_v = 48.6\%$ *Chlorella* suspension acquired in a quiescent state indicates a highly dense distribution of cells that nearly come into a mechanical contact with each other, Fig. 2 (d). Such suspensions of rigid particles that nearly come in contact to each other are often referred to as *random closed packed* suspensions [Krieger and Dougherty(1959), de Kruif et al(1985), Heymann and Aksel(2007)].

Recently, Torquato and his coworkers noted that the two terms *random* and *close packed* are, mathematically speaking, at odds with each other and proposed for this state the term *maximally random jammed state*, [Torquato et al(2000)].

Although it may support the term above, the visual information presented in Fig. 2 (d) is rather minimalistic as it refers to a quiescent state (no flow) and can not fully answer two fundamental questions:

1. Is the viscosity divergence observed at low applied stresses within the **YS** regime related to a cell aggregation under shear or simply to a *maximally random jammed state* microscopic state?
2. Is the flow of the suspension homogeneous within this range of volume fractions and at low applied stresses?

To address these questions we resorted to the in-situ visualisation of the rheometric flow using the Rheoscope module. We have acquired a long sequence (for 60 seconds) of micrographs of a *Chlorella* suspension with a volume fraction $\Phi_v = 0.556$ (the **YS** regime). One such flow image is presented in Fig. 7 (a) (the bright points are *Chlorella* cells which scatter the incoming white light). The images have been acquired at a constant applied stress $\tau = 0.02\ Pa$which lies precisely in the range where the apparent yield stress behaviour is observed. The acquisition of the image sequence allowed one to measure a time series of velocityvfields and calculate the time averaged flow field (see the arrows in Fig. 7 (a)) using the **DPIV** method described in Sec. 2.2. The result of this quantitative assessment is presented in Fig. 7 (b).

A first thing to note is the smallness of the flow speeds (typically smaller $1\mu m/s$) which is consistent with the extremely large values of the measured viscosity (the circles (◯) in Fig. 4).

Secondly, the measurement of the time averaged flow field allows one to indirectly assess the micro-structural organisation of the *Chlorella* suspension by monitoring the regions in the flow field where there exists no measurable flow.

Such regions are highlighted by the closed curves overlapped on each panel of Fig. 7.

The experimental observation of these plug-like flow regions answers both of the questions stated above:

1. The emergence of the apparent yield stress behaviour is related to the formation of large scale particle aggregates that do not move over extended time intervals and ultimately lead to a divergence of the measured viscosity.
2. Corresponding to this state, the flow is highly inhomogeneous. Consequently, the viscosity measurements performed within this regime should be treated as apparent measurements [2]. Unfortunately, the quality and resolution of the flow images acquired with the Rheoscope module did not allow us to analyse the correlation between the local speed, centroids

[2] Note that this strongly inhomogeneous flow field significantly departs from the analytical solution of a cone-plate rheometric flow which allows the accurate conversion of the meassured torque ($T$) and angular speeds ($\Omega$) into stresses ($\tau$) and rates of shear ($\dot{\gamma}$).

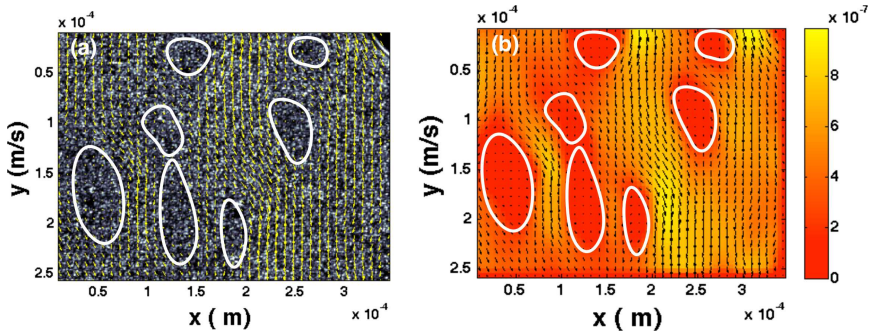


**Fig. 7** **(a)** Micrograph of a *Chlorella* suspension with a volume fraction $\Phi_v = 0.556$ (the **YS** regime) sheared at a stress $\tau = 0.02$ *Pa*. The time averaged velocity field obtained via the **DPIV** method is overlapped onto the image. **(b)** The corresponding time-averaged mean velocity field (the false colour map) and the time averaged velocity vectors. The closed curves superposed to each panel highlight the solid-like agglomerations of *Chlorella* cells.

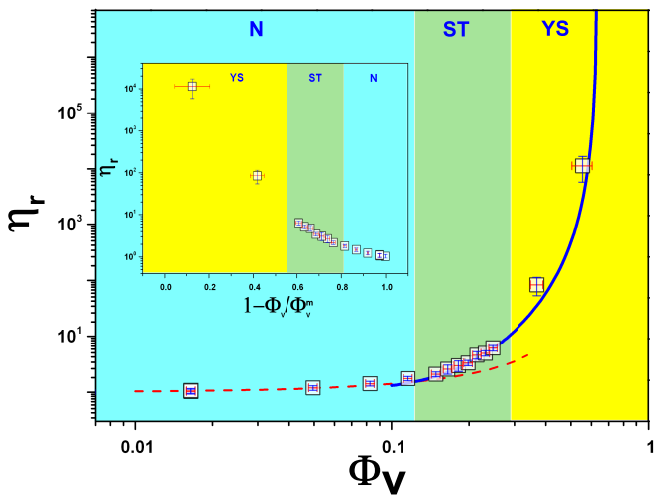


**Fig. 8** Dependence of the relative viscosity of the microalgal suspension $\eta_r$ on the volume fraction of the microalgue $\Phi_V$ . The dashed line is a fit according to the Quemada model [Quemada(1997)] and the full line is a fit according to the Simha model, [Simha(1952)]. The labels indicate the experimentally observed rheological regimes: **N** - Newtonian, **ST** - shear thinning, **YS** - yield stress. Within the **ST** and **YS** regimes, the relative viscosity has been measured at a fixed stress, $\tau = 1Pa$. The same data is re-plotted in the inset versus $1 - \frac{\Phi_v}{\Phi_v}$.

of individual cells and their sizes using the Voronoi triangulation technique previously illustrated in our manuscript. We can only speculate at this point that, as in the case of the cell aggregates (flocs) observed within the **ST** volume fraction regime, the repulsive inter-cell interactions due to the negative interfacial charge of the cell's membrane may play an important role. Future experimental investigation of the microscopic flow and its correlation to the cell distributions are needed to clarify this point.

As in the case of the **ST** volume fraction regime, we have used the Rheoscope module to probe the emergence of the wall slip phenomenon within the **YS** volume fraction regime by monitoring the local flow speed at various depths $z$ within the sample down to the bottom glass plate **GP** (see Fig. 3 (a)). Unlike in the case of the intermediately concentrated **ST** volume fraction regime previously discussed, a significant slip can be observed at the bottom glass plate which, in terms of speeds, accounts up to 30% of the speed of the top cone **C**.

Consequently, separate rheological measurements (data not shown here) performed with a system of rough plates have shown significant differences in a range of small applied stresses. Particularly, the apparent yield stress measured in the presence of slip is several times smaller than that measure with rough geometries. From a fundamental and strictly rheological standpoint, the measurements performed in the presence of wall slip are absolutely unacceptable as they do not reflect true material properties which is the *"golden rheological standard"*.

In an engineering setting, however, this constrain may be somewhat relaxed. As a matter of a fact, realistic fluid motion of microlgae suspensions in intensified photobioreactors occurs in the presence of wall slip. This is simply because the walls of photobioreactors need to be transparent to visible light and, consequently, they are slippery (typically either glass or acrylic made).

In the view of this rather simple and practical argument we believe that, although clearly misleading from a fundamental rheological perspective (particularly if one aims assessing a material property which is beyond the scope of the present work), the viscosity measure-ments we present we present within the **YS** would be quite helpful and instructive in design-ing efficient photobioreactors based on a correct understanding of the in-situ hydrodynamics and rheology and of their practical impact on the mass productivity of the photobioreactors.

Although our rheological data do not suffice to reconstruct a full jamming diagram as proposed in Ref. [Liu and Nigel(1998)] and done in Ref. [Ikeda et al(2012)] which allows one to accurately decouple the jamming and the glass transition, we can obtain a constant temperature section of such a diagram. For this purpose, we turn our attention to the volume fraction dependence of the relative viscosity $\eta_r$ within the various rheological regimes (**N**, **ST**, **YS**) identified above.We monitor the dependence of the relative effective viscosity $\eta_r$ of *Chlorella* microalgae suspensions measured at a constant applied stress $\tau = 1$ *Pa* on the volume fraction $\Phi_v$, Fig.8. To facilitate the comparison of our relative viscosity measurements with previous works by others, we re-plot in the inset of Fig. 8 the same data versus $1 - \frac{\Phi_v}{\Phi_v^m}$.

Within the Newtonian volume fraction regime observed for dilute *Chlorella* suspensions (**N**) the volume fraction dependence of the relative viscosity $\eta_r$ is often modelled by the Quemada model, [Quemada(1997)]:

$$\eta_r = \left(1 - \frac{\Phi_v}{\Phi_v^m}\right)^{-2} \tag{5}$$

The equation above with $\Phi_v^m = 0.637$ can reliably describe the viscosity measurements in the range $\Phi_v \leq 0.115$ (the dotted line in Fig. 8).

Within the concentrated and the highly concentrated regimes (**ST**, **YS**) the volume fraction dependence of the relative viscosity is no longer accurately predicted by the Quemada model. According to the Simha's cellular model [Simha(1952)] which has proven its ability to describe the rheological behaviour of the highly concentrated suspensions, the relative viscosity of the suspension should satisfy:

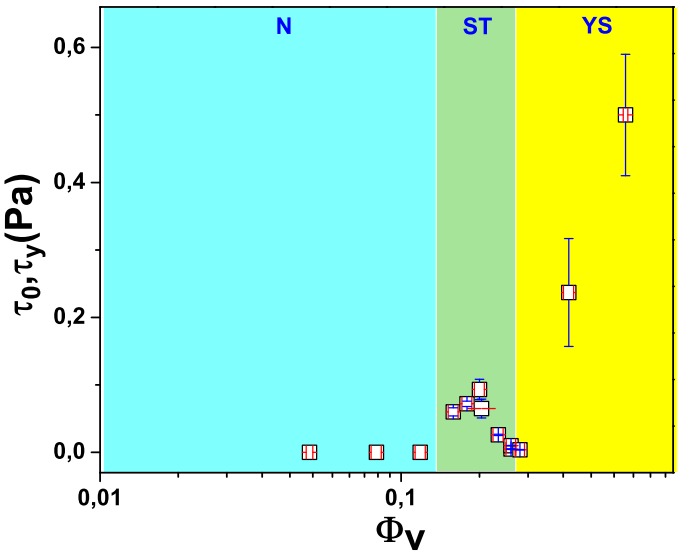


**Fig. 9** Dependence of the onset of the shear thinning behavior $\tau_0$ measured within the **ST** regime and of the apparent yield stress $\tau_y$ on the volume fraction $\Phi_V$. The labels indicate the experimentally observed rheological regimes: **N** - Newtonian, **ST** - shear thinning, **YS** - yield stress .

$$\lim_{\Phi_v \to \Phi_v^m} \eta_r = 1 + \frac{54}{5} f^3 \frac{\Phi_v^2}{\left(1 - \frac{\Phi_v}{\Phi_v^m}\right)^3} \tag{6}$$

where $f$ is a semi-empirical parameter and $\Phi_v^m$ is the maximum packing fraction.

The dependence of the relative viscosity measured at a constant applied stress $\tau = 1Pa$ within the **ST** and **YS** regimes can be fitted by Eq. 6 with $f = 1.2$ and $\Phi_v^m = 0.637$ (the full line in Fig. 8). This value of the maximum packing fraction $\Phi_v^m$ matches closely the theoretical prediction for a *maximally random jammed state*.

The dependence of the onset of the shear thinning behaviour $\tau_0$ and the yield stress $\tau_y$ on the volume fraction $\Phi_v$ is presented in Fig. 9.

Within the shear thinning regime **ST** a non monotone dependence of $\tau_0$ on the volume fraction $\Phi_v$ is observed with a local maximum corresponding to $\Phi_V^c \approx 0.18$ and the corresponding stress value is $\tau_0^c \approx 0.51\Phi_V^c$.

The measurements presented in Fig. 9 are in a good qualitative agreement with the measurements of Kruif and his coworkers, Ref. [de Kruif et al(1985)]. According to Ref. [de Kruif et al(1985)] and [Krieger and Dougherty(1959)]
the maximum stress value $\tau_0^{max}$ reached within the **ST** concentration regime is related to the average cell size via $\tau_0^{max} = \frac{k_b T}{b\overline{r}_0^3}$ where $b$ is the Krieger constant which is independent on the volume fraction. Using $\overline{r}_0 = 1.98\mu m$ (see the distribution of cell size in Fig. 1(b)) and $\tau_0^{max} = 0.09\ Pa$(see Fig. 9) one obtains $b \approx 0.82$ which is of the same order of magnitude with the theoretical value predicted by Krieger ($b = 2.32$), [Krieger and Dougherty(1959)]. The factor of 2 difference between the value we found and the theoretical prediction may be

explained by the fact that the *Chlorella* suspension is not mono disperse (see the statistical distribution presented in Fig. 1(b)).

The similarities of these experimental findings with the rheological behaviour of suspensions at various volume fractions confirms our initial hypothesis that the rheological behaviour of *Chlorella* suspensions may be approached from the perspective of suspensions of rigid particles.

It is known that systems that exhibit a yield stress behaviour may also exhibit irreversibility of the deformation states upon an increase/decrease of the externally applied forcing (thixotropic effects) as well as time dependence of the rheological properties. The next section is dedicated to the investigation of such effects within the **ST** and **YS** regimes identified and characterised through this section.

### 3.2 Reversibility of the deformation states at various microalgae volume fractions

To probe the reversibility of the deformation states, linear (in time) controlled stress flow ramps are performed for both increasing and decreasing stresses. Each of the explored stress values is maintained constant for a time $t_0$ referred to as the *characteristic forcing time* (see Fig. 3(b)).

The reversibility of the deformation states within the intermediate concentration regime (the **ST** regime) has been probed by comparing viscosity measurements performed on increasing and decreasing stress ramps for several characteristic forcing times $t_0$, Fig. 10.

Regardless the value of the characteristic forcing time, on the increasing branch of the stress ramp (the squares (□) in Fig. 10) two deformation regimes are observed:

1. A Newtonian like regime characterized by a viscosity plateau at low values of the applied stresses. According to [Quemada(1997)], this regime may be understood in terms of a mesoscopic organization of single cells into flocs of cells.
2. An entirely de-structured regime at high values of the applied stresses. Within this regimes the cells mesostructures are destroyed by shear which translates into a lower viscosityplateau.

   Upon a decrease of the applied stresses (the circles (◯) in Fig. 10), the deformation states are recovered only within the entirely de-structured (fluid) regime.

For each value of the characteristic forcing time $t_0$ investigated, the system does not return to a mesoscopic floc structure but collapses into a large scale cell network characterised by a viscosity which diverges at low stresses. Bearing in mind that this range of microalgae volume fractions lies significantly below the maximum packing fraction $\Phi_v^m$ and thus individual *Chlorella* cells do not jam (see panels (b,c) in Fig. 2), the observation of a viscosity divergence on the de-creasing stress branch and at low applied stresses appears to us quite puzzling and deserves a brief discussion. Within the intermediate range of volume fractions the average inter-cell distance may become of the same order of magnitude with the Debye length and thus, an effective repulsive force network leads to the viscosity divergence in a range of low applied stresses observed in Fig. 10. It remains, however, to be clarified by future investigations why such a viscosity divergence is observed only on the decreasing branch of the stress ramp.

Viscosity measurements performed on a microalgae suspension with a volume fraction $\Phi_v = 0.556$ (within the **YS** regime, see Fig. 8) for an increasing and a decreasing linear stress ramp are presented in Fig. 11.

As already illustrated in Fig. 4 and discussed above, within the highly concentrated regime **YS** a viscosity divergence is observed in a range of small stresses on both the in-creasing branch of the stress ramp (the squares (□) in Fig. 11) and the decreasing one

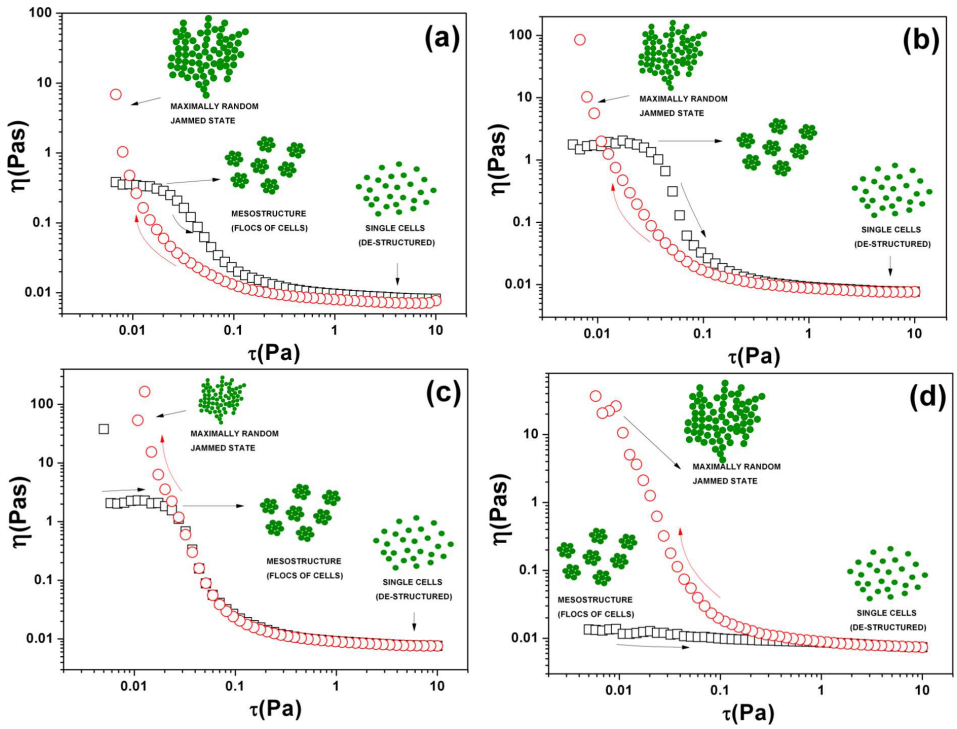


**Fig. 10** Viscosity measurements within the intermediate concentration regime at a volume fraction $\Phi_v = 0.148$ (**ST**, see Fig. 8) for both increasing (□) and decreasing (○) stress ramp and several values of the characteristic forcing time: **(a)** $t_0 = 5\ s$ **(b)** $t_0 = 10\ s$ **(c)** $t_0 = 15\ s$ **(d)** $t_0 = 30\ s$.

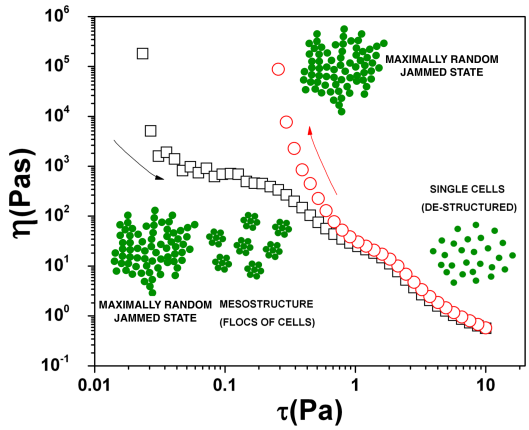


**Fig. 11** Viscosity measurements within the highly concentrated regime at a volume fraction $\Phi_v = 0.556$ (the **YS** regime, see Fig. 8) for both increasing (□) and decreasing (○) stress ramp. The characteristic forcing time was $t_0 = 15s$.

the circles (◯) in Fig. 11). The viscosity divergence can be understood in terms of a jammed particle network extended over the entire sample. This behaviour is consistent with the mi-cro structural information presented in Fig. 2 (d) which clearly indicates that neighbouring *Chlorella* cells come into contact.

As the applied stress is increased along the increasing branch of the stress ramp, a gradual transition towards liquid states (the microalgae suspension is completely de-structured) is observed. The cell network responsible for the yield stress behaviour depicted in Fig. 11 breaks down into a suspension of flocs of cells (mesoscopic cell structure). Within this intermediate state, a viscosity plateau is observed, similar to the low stress Newtonian plateau observed at intermediate volume fractions within the **ST** rheological regime. As the applied stress is increased even further, the flocs of cells break down and a shear thinning fluid state is observed.

Upon a decrease of the applied stresses (the ”down” branch of the stress ramp) the defor-mation states are recovered only within the fluid regime. We note that no intermediate vis-cosity plateau is observed on the decreasing stress branch: the system passes directly from a de-structured state to a cell network state characterised by a divergent viscosity. A similar ir-reversible solid-fluid transition has been recently observed for a PMMA suspension by Hey-mann and Aksel, [Heymann and Aksel(2007)]. As stated in Ref. [Heymann and Aksel(2007)], the emergence of a hysteresis clearly indicates that the static and dynamic structures of cells are quite different at the same low applied stress of the up and down branches of the flow curve.

Individual inspection of various increasing/decreasing flow ramps measured within both the **ST** and **YS** regimes indicates that there exists an onset of irreversibility of the deformation states which, most probably, corresponds to the complete breakdown of cell structures (flocs). Unfortunately, for the case of *Chlorella* microalgae, we are not aware of a theoretical framework able to describe this by accounting not only for the hydrodynamic interactions but for the electrostatic repulsions as well.

The irreversible (hysteretic) solid-fluid transition of the highly concentrated *Chlorella* microalgae suspension under shear also bears some similarities with the solid-fluid transition recently observed in a shear thinning physical gel (Carbopol), [Putz and Burghelea(2009)]. We note, however, that the solid behaviour visible in Fig. 11 is not necessarily related to elasticity, as it was the case for the physical gel studied in [Putz and Burghelea(2009)].

A irreversible flow behaviour strikingly similar to that depicted in Fig. 11 has been ob-served by Malkin and his coworkers, [Malkin et al(2004)], on an super-concentrated water in oil (WO) emulsion. They interpret the viscosity increase on the decreasing stress branch in the range of low shear rates as a rheopectic effect induced by the ageing of the emulsion.

These unexpected similarities between the yielding scenario in various micro structurally different systems suggest that the solid-fluid transition in soft materials may follow a universal pattern related to the competition between formation and destruction of flow units.

The irreversibility of deformation states is usually associated with thixotropic or time dependent effects in the rheological behaviour. To explore this, we focus on the dependence of the viscosity measured at a fixed applied stress on the characteristic forcing time $t_0$. The results of such measurements for three values of the volume fraction $\Phi_v$ corresponding to the **ST** regime are presented in Fig. 12.

Up to a critical value of the characteristic forcing time $t_0 \approx 15\ s$ which is of the same order of magnitude with the characteristic time scale associated with the Brownian motion

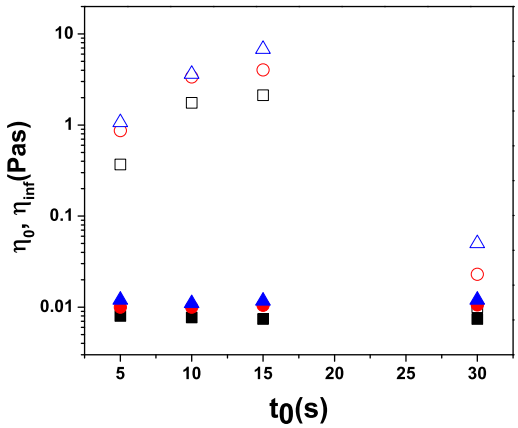


**Fig. 12** Dependence of the zero shear viscosity $\eta_0$ (empty symbols) and the terminal viscosity $\eta_{int}$ (full sysmbols) measured within the **ST** regime on the increasing branch of the stress ramp on the characteristic time of forcing $t_0$. The symbols refer to different volume fractions of the microalgae: (□, ■) - $\Phi_v = 0.148$,(◯, ●) - $\Phi_v = 0.165$, (△, ▲) - $\Phi_v = 0.181$.

$t_{br}$ (or $De \approx 1$) [3], the zero shear viscosity (the empty symbols in Fig. 12) increases almost an order of magnitude. This viscosity increase in conjunction with the micro structural picture illustrated in Fig. 2(d) indicates that smaller the Deborah number is, larger is the characteris-tic size of structured flocs of *Chlorella* cells. For values of $t_0$ larger than $t_{br}$ a drop of nearly two orders of magnitude of the zero shear viscosity is observed indicating for large waiting times the rate of formation of flocs of cells is overcome by the rate of destruction induced by the shear. Although we have checked the reproducibility of this effect during subsequent experiments performed on different batches of suspensions, we are unable at this point to provide a full physical interpretation of this effect. Measurements of the high shear plateau viscosity $\eta_{int}$ (the full symbols in Fig. 12) indicate no dependence on the characteristic forcing time $t_0$ which indicates that in a fully destructured deformation regime no time dependent effect are present. This finding is fully consistent with the reversibility of the deformation states observed in a range of large applied stresses, Fig. 10. Measurements of the viscosity of a highly concentrated microalgae suspension (the regime **YS** in Fig. 8) at a given applied stress as a function of the characteristic forcing time $t_0$ are presented in Fig. 13. Depending on the value of the applied stress, two behaviours with respect to the char-acteristic forcing time are found. For $\tau = 10Pa$ which corresponds to the reversible fluid deformation regime (see Fig. 11), no significant variation of the viscosity with $t_0$ can be observed (the full symbols in Fig. 13). This indicates that, corresponding to this value of the applied stress the entire sample is in a liquid state and no re-structuration of the microalgae suspension occurs. This conclusion is consistent with the reversibility of the flow curved observed within the fluid regime, Fig. 11. The dependence of the viscosity on the characteristic forcing time is significantly different, however, for a low value of the applied stresses ($\tau = 0.1Pa$). Within this deformation

[3] Note that if one takes into account the measured average cell radius and its standard deviation one obtains $t_{br} \in [16.4, 65.7]\ s$ (see Fig. 1 and the discussion in Sec. 2.1).

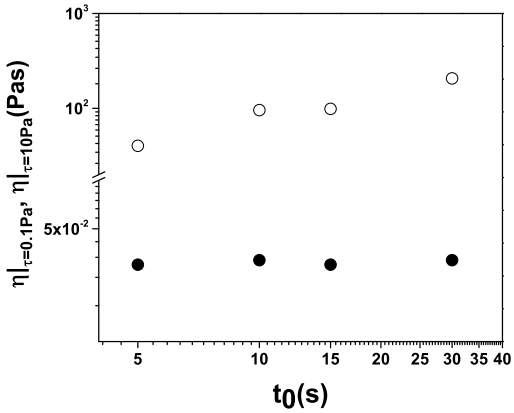


**Fig. 13** Dependence of the viscosity of a highly concentrated suspension (within the **YS** rheological regime, ) measured at a fixed stress on the characteristic forcing time. The symbols refer to stress value: (◯) - $\tau = 0.1Pa$, (●) - $\tau = 10Pa$ .The volume fraction is $\Phi_v = 0.37$.

regime, a monotone increase of the viscosity with the characteristic forcing time is observed (the empty symbols in Fig. 13).

This observation, in conjunction with the visualisation of the rigid plugs formed by large scale agglomerations of individual cells presented in Fig. 7 indicates that average size of these agglomerations decreases monotonically with the Deborah number, *De*. In other words, steadier the flow is, more likely is that the *Chlorella* cells form large plug-like zones gradually leading to a *maximally random jammed state* manifested by a divergence of the apparent viscosity.

A similar time dependent rheological behaviour has recently been observed by Schmidt and Münstedt [Schmidt and Münstedt(2002)] for concentrated monodisperse suspensions. They have observed a strong dependence of the rheological properties (zero shear viscosity and dynamic moduli) of the suspensions on the pre-shear time. The zero shear viscosity was found to increase with increasing pre-shear time which they interpret by structuring effects. In contrast to the loss modulus, which has not been influenced significantly by pre-shear, the storage modulus increased substantially with increasing pre-shear times at low angular frequencies. This was interpreted as a transition from a liquid-like to a solid-like viscoelastic structure of the particle network.

## 4 Conclusions, outlook

A systematic study of the rheological behaviour of suspensions of non-swimming microalgae is presented. Depending on the microalgae volume fraction, three distinct rheological regimes are observed. At low volume fractions ($\Phi_v < 0.115$) a Newtonian regime (**N**) is ob-served: the viscosity is independent on the applied stress and the flow curves are reversible upon an increase/decrease of the applied stresses.

At larger volume fractions ($0.115 < \Phi_v < 0.25$), a shear thinning **ST** regime is observed. At low values of the applied stresses a Newtonian viscosity plateau is observed. We interpret this plateau in terms of a meso-structure of *Chlorella* cells (flocs). As the applied stress exceeds a critical value, a strong shear thinning behaviour is observed, which corresponds to

a progressive breakdown of the meso-structure. A complete destruction of the mesostructure in a range of large applied stresses results in a second viscosity plateau, $\eta_{inf}$.

The microscopic scale picture responsible for the observation of a low shear viscosity plateau is demonstrated by visualisation of the *Chlorella* suspension. Using the Voronoi triangulation technique, we have demonstrated in the absence of flow ($\tau \to 0$) the formation of flocs of small cells and the occurrence of voids around the larger ones, Fig. 5.

This somewhat unexpected microscopic scale organisation of individual *Chlorella* cells can be explained in terms of repulsive interactions due to their negative superficial charge which is proportional to the square of the cell's radius. The large cells carry a larger superficial charge and repel strongly the smaller ones creating voids around them. Consequently, the smaller cells are organised in flocs.

A similar observation is made in the presence of shear for stress values corresponding to the low shear viscosity plateau $\tau < \tau_0$, Fig. 6.

For the highest volume fractions investigated ($\Phi_v > 0.25$) a apparent yield stress regime **YS** characterised by a divergence of the viscosity at low stresses is observed. The emergence of an apparent yield stress behaviour is interpreted in terms of the formation of large scale cell aggregates which, in the limit of small applied stresses, behave as rigid plugs leading to a viscosity divergence, Fig. 7. The time series of velocity field acquired within this range of volume fractions and applied stresses indicates that these plug-like zones persist over significant times.

The volume fraction dependence of the viscosity measured at a fixed applied stress (within the fluid deformation regime) follows the Quemada correlation within the **ST** regime and the Simha correlation within the **YS** regime, Fig. 8. As both above mentioned theoret-ical models refer to suspensions of non-interacting particles and bearing in mind that the repulsive interactions among individual *Chlorella* is not negligible the rather unexpected agreement of our relative viscosity data with their prediction is certainly worth being further investigated by both macro and micro rheology approaches.

The dependencies of the onset of the shear thinning behavior $\tau_0$ and the apparent yield stress $\tau_y$ presented in Fig. 9 are consistent with the previous results obtained for suspensions of hard spheres, [de Kruif et al(1985), Tropea et al(2007)].

This indicates that, quite surprisingly and in spite of the relative poly-dispersity and the inter-cell repulsive interactions, the rheological behaviour of microalgal suspensions of *Chlorella* can be approached (at least formally) within the framework of non-Brownian suspensions of rigid and non-interacting particles.

Within the semi-concentrated **ST** and the highly concentrated **YS** volume fraction regimes the deformation regimes are not reversible upon increasing/decreasing the applied stresses (except in a range of large applied stresses where the *Chlorella* suspension is fully destructured), Figs. 10, 11. This rather unexpected (and, to our best knowledge, not docu-mented by previous studies) thixotropic like behaviour suggests that before realistic numeri-cal simulations of the hydrodynamic behaviour in photobioreactors could be carried on, new rheological models need to be developed. For such models to be successfully developed a better understanding of the mesoscopic scale interactions and organisation of *Chlorella* cells under shear is needed.

Simultaneously with the thixotropic-like behaviour observed within the **ST** and **YS** regimes a time dependence of the viscosity measured at a fixed applied stress is observed, Figs. 12, 13. This finding as well calls for future investigations from both a theoretical and a experimental perspective.

To conclude, our experimental study has presented a detailed account of the dependence of the rheological behaviour of a *Chlorella* suspensions on the Péclet number *Pe* (controlled

by the rate of shear $\dot{\gamma}$), the Deborah number *De* (controlled by the characteristic forcing time $t_0$) and the volume fraction $\Phi_v$. The reach phenomenology observed by varying the volume fraction in a broad range should certainly call for future studies targeting both a new theoretical framework and the microscopic origins of the experimentally observed features. Based on such studies, the ultimate goal would be to develop suitable numerical codes able to predict the productivity of photobioreactors in relation to both various illumination conditions (fluxes, spectral content, incidence angles) and flow conditions.

**Acknowledgements** This work was supported by the PERLE 2 (Pôle Émergent pour la Recherche Ligèrienne en Énergie) program generously funded by the *Pays de la Loire* district.

We gratefully acknowledge the technical support of Dr. Philippe Sierro and Mr. Etienne Roussel from Thermo Fisher Scientific, Karlsruhe, Germany for the calibration of the nano-torque module installed on the Mars III rheometer and for the optimisation of the Rheoscope module.

T. B. gratefully acknowledges enlightening discussions with Miguel Moyers-Gonzalez.

A. S., J. P. and J. L. are grateful to M. Frappart for providing a large quantity of algae suspensions and to D. Grizeau for his precious insights on the algae structure.

Last but not least, we are particularly indebted to the anonymous referees for their enlightening comments, remarks and suggestions.

## References

Adesanya, Vadillo, and Mackley. Adesanya VO, Vadillo DC, Mackley MR (2012) The rheological characterization of algae suspensions for the production of biofuels. Journal of Rheology 56(4):925-939

Basu H, Vecchio A, Flider F, Orthoeter F (2001) Nutritional and potential disease prevention properties of carotenoids. Journal of the American Oil Chemists' Society 78:665–675

Becker W (2007) Microalgae in Human and Animal Nutrition. Blackwell Publishing Ltd.

de Berg, Cheong, van Kreveld, and Overmars (2008) Computational Geometry: Algorithms and Applications. Springer-Verlag Berlin and Heidelberg GmbH

Buscall R (2010) Letter to the editor: Wall slip in dispersion rheometry. Journal of Rheology 54(6):1177–1183,

Carvalho AP, Meireles LA, Malcata FX (2006) Microalgal reactors: A review of enclosed system designs and performances. Biotechnology Progress 22(6):1490–1506,

Cornet JF (2010) Calculation of optimal design and ideal productivities of volumetrically lightened photobioreactors using the constructal approach. Chemical Engineering Science 65(2):985 – 998,

Cross MM (1965) Rheology of Non-Newtonian fluids: a new flow equation for pseudoplacstic systems. Journal of Colloid Science 20:417 – 437

Dibble CJ, Kogan M, Solomon MJ (2006) Structure and dynamics of colloidal depletion gels: Coincidence of transitions and heterogeneity. Phys Rev E 74:041,403,

Doucha J, Straka F, Livansky K (2005) Utilization of flue gas for cultivation of microalgae *Chlorella* sp.) in an outdoor open thin-layer photobioreactor. Journal of Applied Phycology 17:403–412,

Harris E (1989) The Chlamydomonas Sourcebook : a comprehensive guide to biology and laboratory use. Academic Press Inc. San Diego.

Heymann L, Aksel N (2007) Transition pathways between solid and liquid state in suspensions. Phys Rev E 75:021,505

Ikeda A, Berthier L, Sollich P (2012) Unified study of glass and jamming rheology in soft particle systems. Phys Rev Lett 109:018,301,

Jaishankar, Sharma, and McKinley. Jaishankar A, Sharma V, McKinley GH (2011) Interfacial viscoelasticity, yielding and creep ringing of globular protein-surfactant mixtures. Soft Matter 7:7623–7634,

Kapaun E, Reisser W (1995) A chitin-like glycan in the cell wall of a chlorella sp. (chlorococcales, chlorophyceae). Planta 197:577–582,

Krieger IM, Dougherty TJ (1959) A mechanism for non-newtonian flow in suspensions of rigid spheres. Trans Soc Rheol 3:137

de Kruif, van Iersel, Vrij, and Russel. de Kruif CG, van Iersel EMF, Vrij A, Russel WB (1985) Hard sphere colloidal dispersions: Viscosity as a function of shear rate and volume fraction. The Journal of Chemical Physics 83(9):4717–4725

Kumar, Yadava, and Gaur. Kumar H, Yadava P, Gaur J (1981) Electrical floccula-tion of the unicellular green alga chlorella vulgaris beijerinck. Aquatic Botany 11(0):187 – 195,

Lehr F, Posten C (2009) Closed photo-bioreactors as tools for biofuel production. Current Opinion in Biotechnology 20(3):280 – 285,

Liu AJ, Nigel SR (1998) Nonlinear dynamics: Jamming is not just cool any more. Nature (London) 396:21

Malkin, Masalova, Slatter, and Wilson. Malkin AY, Masalova I, Slatter P, Wilson K (2004) Effect of droplet size on the rheological properties of highly-concentrated w/o emulsions. Rheo-logica Acta 43:584–591

Mata, Martins, and Caetano. Mata TM, Martins AA, Caetano NS (2010) Microalgae for biodiesel production and other applications: A review. Renewable and Sustainable Energy Reviews 14(1):217–232,

Mouget JL, Tremblin G (2002) Suitability of the fluorescence monitoring system (fms, hansatech) for measurement of photosynthetic characteristics in algae. Renewable and Sus-tainable Energy Reviews 74:219–231

Mueller S, Llewellin EW, Mader HM (2010) The rheology of suspensions of solid particles. Proceedings of the Royal Society A 466:1201 – 1228

Northcote H D, Goulding J K (1958) The chemical composition and structure of the cell wall of *Chlorella pyeroidosa*. Biochemical Journal 70(3):391–397

Pandey A, Larroche C, Ricke SC, Dussap C (2011) Biofuels: Alternative Feedstocks and Conversion Processes, Academic Press, chap 19

Pottier L (2005) Modélisation de photobioréacteurs pour la valorisation des microalgues. PhD thesis, University of Nantes

Putz AMV, Burghelea TI (2009) The solid-fluid transition in a yield stress shear thinning physical gel. Rheologica Acta 48(6):673–689

Quemada D (1997) Rheological modelling of complex fluids. i. the concept of effective volume fraction revisited. The European Physical Journal - Applied Physics 1:119–127

Raffel M, Willert CE, Wereley ST,Kompenhans J (September 2007) Particle Image Velocimetry: A Practical Guide (Experimental Fluid Mechanics). Springer; 2nd edition

Richmond A (2004) Principles for attaining maximal microalgal productivity in photo-bioreactors: an overview. In: Ang PO, Dumont HJ (eds) Asian Pacific Phycology in the 21st Century: Prospects and Challenges, Developments in Hydrobiology, vol 173, Springer Netherlands, pp 33–37

Satyanarayana, Mariano, and Vargas. Satyanarayana KG, Mariano AB, Vargas JVC (2011) A review on microalgae, a versatile source for sustainable energy and materials. Interna-tional Journal of Energy Research 35(4):291–311,

Scarano F, Rhiethmuller ML (2001) Advances in iterative multigrid piv image processing. Exp Fluids 29

Schmidt M, Münstedt H (2002) Reological behaviour of concentrated monodisperse suspensions as a function of preshear conditions and temperature: an experimental study. Rheologica Acta 41:193–204

Shi XM, Chen F, Yuan JP, Chen H (1997) Heterotrophic production of lutein by selected chlorella strains. Journal of Applied Phycology 9:445–450

Simha R (1952) A treatment of the viscosity of concentrated suspensions. Journal of Applied Physics 23:1020 – 1024

Spolaore, Joannis-Cassan, Duran, and Isambert. Spolaore P, Joannis-Cassan C, Duran E, Isambert A (2006) Commercial applications of microalgae. Journal of Bioscience and Bioengineering 101(2):87 – 96,

Takeda H (1988) Classification of chlorella strains by means of the sugar components of the cell wall. Biochemical Systematics and Ecology 16(4):367 – 371, ,

Torquato, Truskett, and Debenedetti. Torquato S, Truskett TM, Debenedetti PG (2000) Is random close packing of spheres well defined? Phys Rev Lett 84:2064–2067, DOI 10.1103/PhysRevLett.84.2064,

Tropea, Yarin, and Foss. Tropea C, Yarin AL, Foss JS (2007) Handbook of experimental fluid dynamics. Springer-Verlag, Berlin Heidelberg

Ugwu, Aoyagi, and Uchiyama. Ugwu C, Aoyagi H, Uchiyama H (2008) Photobioreactors for mass cultivation of algae. Bioresource Technology 99(10):4021 – 4028, Wagner J Norman J Mewis (2011) Colloidal Suspension Rheology. Cambridge University Press

Wileman, Ozkan, and Berberoglu. Wileman A, Ozkan A, Berberoglu H (2011) Rheological properties of algae slurries for minimizing harvesting energy requirements in biofuel production. Bioresource Technology

Wu ZY, Shi XM (2008) Rheological properties of *Chlorella pyrenoidosa* culture grown heterotrophically in a fermentor. Journal of Applied Phycology 20:279–282